

Magneto-induced topological phase transition in inverted InAs/GaSb bilayers

Zhongdong Han^{1,*}, Tingxin Li^{1,†}, Long Zhang^{2,4} and Rui-Rui Du^{1,3,4,‡}

¹International Center for Quantum Materials, School of Physics, Peking University, Beijing 100871, China

²Kavli Institute for Theoretical Sciences and CAS Center for Excellence,
University of Chinese Academy of Sciences, Beijing 100190, China

³Collaborative Innovation Center of Quantum Matter, Beijing 100871, China

⁴Hefei National Laboratory, Hefei 230088, China



(Received 13 January 2023; revised 2 January 2024; accepted 3 April 2024; published 20 May 2024)

We report a magneto-induced topological phase transition in inverted InAs/GaSb bilayers from a quantum spin Hall insulator to a normal insulator. We utilize a dual-gated Corbino device in which the degree of band inversion, or equivalently the electron and hole densities, can be continuously tuned. We observe a topological phase transition around the magnetic field where a band crossing occurs, accompanied by a bulk-gap closure characterized by a bulk conductance peak (BCP). In another set of experiments, we study the transition under a tilted magnetic field (tilt angle θ). We observe the characteristic magnetoconductance around BCP as a function of θ , which dramatically depends on the density of the bilayers. In a relatively deep inversion (hence a higher density) regime, where the electron-hole hybridization dominates the excitonic interaction, the BCP grows with θ . On the contrary, in a shallowly inverted (a lower density) regime, where the excitonic interaction dominates the hybridization, the BCP is suppressed indicating a smooth crossover without a gap closure. This suggests the existence of a low-density, correlated insulator with spontaneous symmetry breaking near the critical point. Our highly controllable electron-hole system offers an ideal platform to study interacting topological states as proposed by recent theories.

DOI: [10.1103/PhysRevResearch.6.023192](https://doi.org/10.1103/PhysRevResearch.6.023192)

I. INTRODUCTION

The quantum spin Hall insulator (QSHI) is a topologically non-trivial state described by a Z_2 topological invariant [1]. It supports a bulk gap and dissipationless helical states along the edge. Several candidate materials have been experimentally confirmed to host the QSH phase, including HgTe/CdTe [2] and InAs/GaSb quantum wells (QWs) [3], 1T'-WTe₂ monolayer [4], and potentially transition metal dichalcogenide moiré systems [5]. The physics of the QSH states can be well captured with the Bernevig-Hughes-Zhang (BHZ) model [6] or the Kane-Mele model [7] in the single-particle paradigm. However, an observation in InAs/GaSb bilayer [8]—the persisting conductance quantization up to a 12 T in-plane magnetic field—challenges the single-particle picture, which catches more attention on many-body interaction in such systems and opens up an opportunity to study

topological excitonic insulators [9]. Recent theoretical works [10–13] show that topology, correlation, and their interplay can lead to an abundance of exotic states of matter unexplored so far, with the underlying physics being described by correlation-driven spontaneous symmetry breaking. As is common in condensed matter systems, the resulting phase diagram becomes richer and more interesting as an electron-hole bilayer is subject to a magnetic field. Despite some previous experiments under magnetic fields as reported in, e.g., [2,14], no attention was paid to the evidence of Coulomb interaction in those reports. Part of the reason may be that in those deeply inverted InAs/GaSb and HgTe/CgTe QWs studied, the electron-hole (e - h) hybridization dominates and the Coulomb interaction U is nearly negligible compared to the tunneling strength A [15,16]. However, because of the dominance of excitonic interaction over the hybridization, shallowly inverted InAs/GaSb QWs provide an ideal platform to study those correlation-induced phases. In this paper, we demonstrate topological phase transitions from a QSHI to a normal insulator (NI) in an inverted InAs/GaSb bilayer under either a perpendicular or a tilted magnetic field.

II. DEVICE AND MEASUREMENT

InAs/GaSb bilayer is a broken-gap type-II heterostructure where the InAs conduction band is lower than the GaSb valence band by about 150 meV. Intuitively, a straightforward approach to realize a phase transition from a QSHI to a NI is engineering the band crossing. The perpendicular

*Present address: Laboratory of Atomic and Solid State Physics, Cornell University, NY 14850, USA; zh352@cornell.edu

†Present address: Key Laboratory of Artificial Structures and Quantum Control (Ministry of Education), School of Physics and Astronomy, Shanghai Jiao Tong University, Shanghai 200240, China.

‡rrd@pku.edu.cn

Published by the American Physical Society under the terms of the [Creative Commons Attribution 4.0 International](https://creativecommons.org/licenses/by/4.0/) license. Further distribution of this work must maintain attribution to the author(s) and the published article's title, journal citation, and DOI.

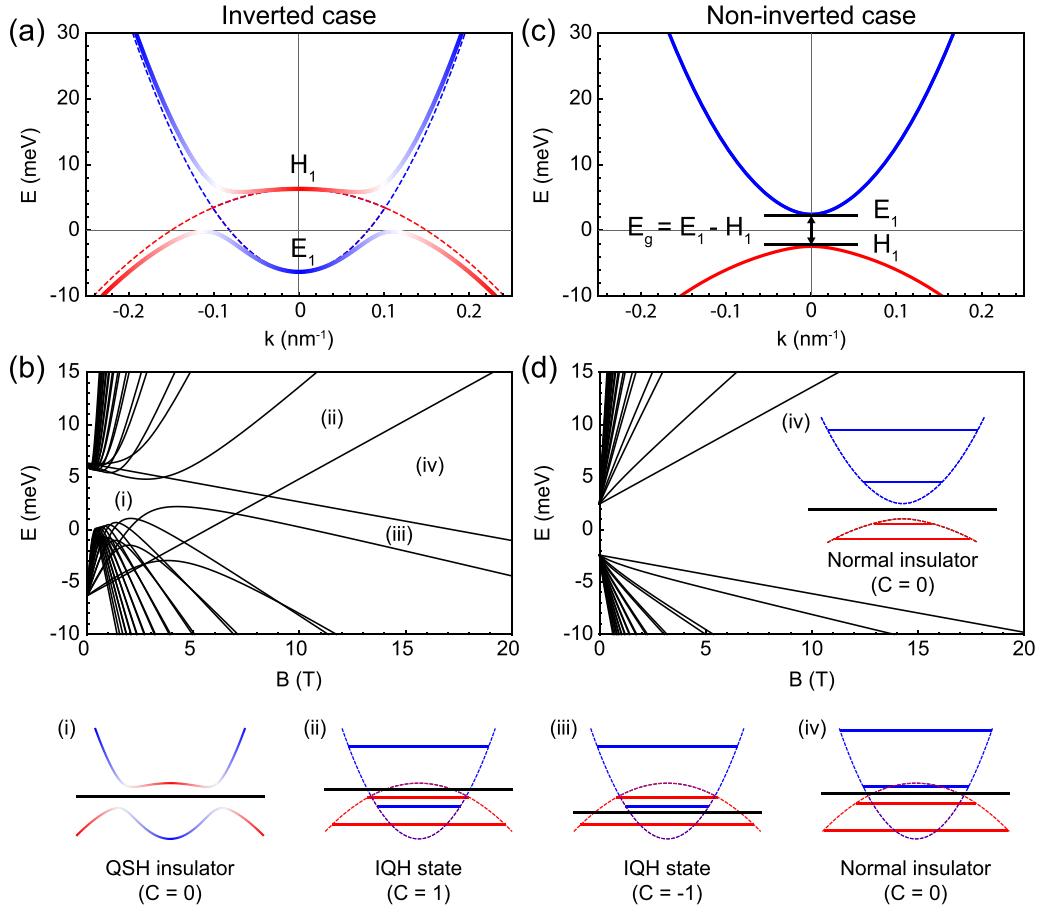


FIG. 1. (a) Energy dispersion of type-II InAs/GaSb QWs with an inverted band structure based on a noninteracting model. The dashed lines describe the dispersion without hybridization, where E_1 and H_1 denote the electron and hole bands, respectively. (b) LL spectra for the inverted case in (a). Two unhybridized LLs divide the region in the vicinity of the inversion transition into four regimes with different Chern numbers labeled (i)–(iv). Corresponding schematics of the band structures are plotted below: (i) a QSHI state with an inverted band order with the Chern number $C = 0$; (ii) a QH state with only the lowest electron LL occupied ($C = 1$); (iii) a QH state with only the lowest hole LL occupied ($C = -1$); (iv) a QH state with no occupation in LLs ($C = 0$), namely, a normal insulator, where the blue (red) lines denote the electron (hole) LLs and the black lines represent the chemical potentials. (c) Energy dispersion and (d) LL spectra for a noninverted case.

magnetic field is an effective knob for tuning the band alignment due to the orbital effect. Without considering the Coulomb interaction, the band crossing transition should be a topological phase transition accompanied by a bulk gap closure between these two insulating states. On the other hand, in the dilute limit [9] the reduced screening makes the Coulomb interaction dominate the hybridization. Dual-gated geometry offers *in situ* and continuous tunability of the effective interaction strength (U/A), which can also be tuned by applying an in-plane magnetic field.

Here we focus on low-temperature bulk transport properties measured from a dual-gated Corbino device, which excludes the edge contribution [8]. Contrary to a Hall mesa, only the bulk contributes to the conductivity which enables us to study the magnetotransport of the system purely from the bulk. Our high-quality bilayer samples are grown by semiconductor molecular beam epitaxy technique. The detailed structure can be found in the Supplemental Material [17]. Dual-gated configuration makes the system highly controllable, allowing independent tuning of both the Fermi energy and the band inversion.

Our measurements are performed in ³He refrigerators. All data are taken at 300 mK unless specified otherwise. Standard pseudo-four-terminal methods with low-frequency (13.7 Hz) and low-excitation (1 mV) lock-in techniques are adopted in data collection.

III. PHASE DIAGRAM UNDER PERPENDICULAR B FIELD

Figure 1 shows band structures under different conditions calculated by the two-band BHZ model [6,18]. The electron and hole effective masses are taken from experiments [19]. The crossing density $n_{\text{cross}} = 1.63 \times 10^{11} \text{ cm}^{-2}$, which characterizes the band inversion $E_g = \pi \hbar^2 n_{\text{cross}} (1/m_e^* + 1/m_h^*)$, is estimated from the analysis of the in-gap oscillations [20]. The bulk inversion asymmetry (BIA) and structure inversion asymmetry (SIA) are not considered here because those effects are normally small [21].

Figures 1(a) and 1(b) present the band dispersion and Landau level (LL) spectra for an inverted case. It represents a simple semimetal, as depicted by dashed lines in Fig. 1(a), if we turn off the band hybridization. Under a uniform

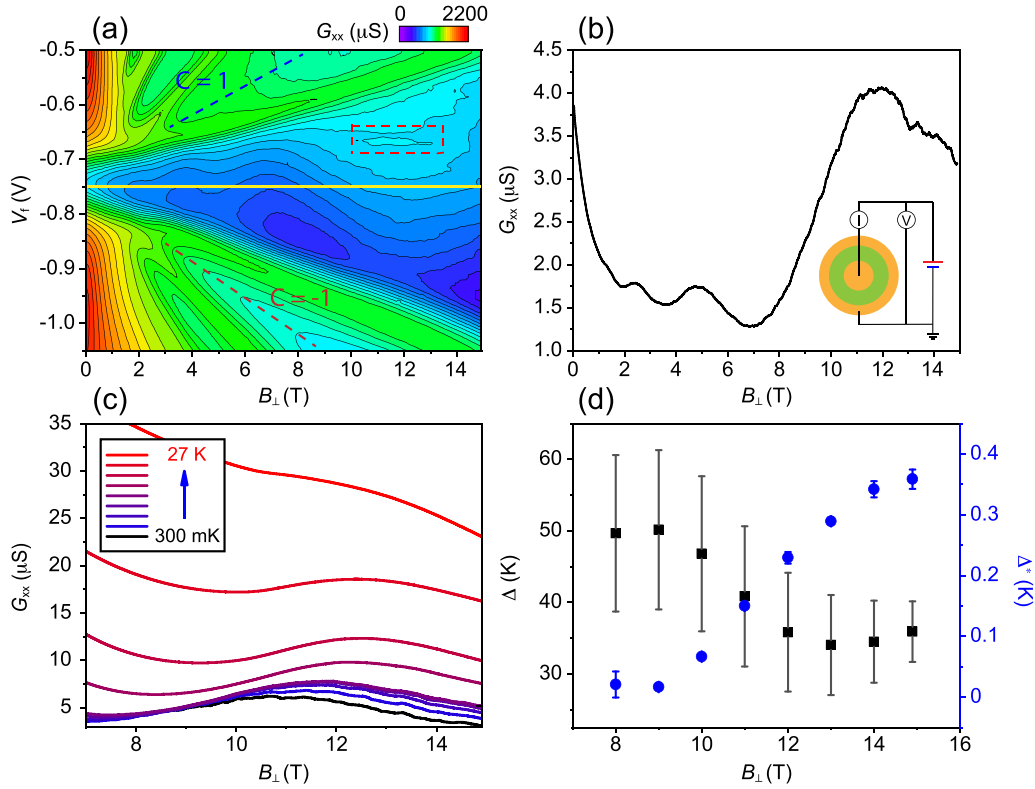


FIG. 2. (a) Bulk conductivity as a function of V_f and B_{\perp} at $V_b = 0$ V. The conductivity is measured from a dual-gated Corbino device. The red dashed-line box marks a bulk conductance peak around 12 T. The blue (red) dashed line denotes the IQH state with Chern number $C = 1$ ($C = -1$) as described in Fig. 1(b). The magnetoconductance trace is plotted in (b) where the Fermi energy is pinned at the CNP ($V_f = -0.75$ V, yellow line in the contour plot). (c) The temperature dependence of the bulk conductance peak near the transition point at the CNP. (d) The energy gap vs perpendicular magnetic field acquired by the Arrhenius analysis from the data in (c). The energy gap Δ shows a minimum around 13 T accompanied by the opening of a small gap Δ^* .

magnetic field, there exist two sets of LLs. The perpendicular magnetic field leads to a relative shift of the electron and hole bands in energy, tuning the band structure from an inverted order to a normal (noninverted) order. This conclusion remains valid even after the hybridization is resumed. The difference is that the hybridization converts the semimetal into a topologically nontrivial QSHI at zero magnetic field. As shown in Fig. 1(b), it leads to anticrossings of electron and hole LLs except the lowest Landau levels (LLs) [16,22]. The only remaining crossing point determined by these two unhybridized LLs reveals a topologically protected gap closure during the phase transition from a (topologically nontrivial) QSHI to a (topologically trivial) NI. Though the time-reversal symmetry is broken in high magnetic fields, this topological phase transition is still protected by other symmetries, such as the spatial mirror symmetry [23,24] due to the vanishingly small BIA and SIA in the InAs/GaSb system [21].

For comparison, for a normal band structure with a non-inverted order—the conduction band is higher in energy than the valence band—the topology is trivial. As shown in Figs. 1(c) and 1(d), the magnetic field pulls the electron and hole LLs apart from the charge neutrality point (CNP) but neither changes the band order nor results in a phase transition.

IV. TOPOLOGICAL PHASE TRANSITION FROM A QSHI TO A NI

Figure 2(a) shows the bulk conductivity as a function of the front-gate voltage V_f and the magnetic field B_{\perp} at the back-gate voltage $V_b = 0$ V. The conductance shows a dip at $V_f = -0.75$ V under zero magnetic field, indicating the position of the CNP. When fixing the Fermi energy at the CNP, the conductivity in Fig. 2(b) shows clear quantum oscillations, which are followed by a pronounced, broad BCP around 12 T. The in-gap quantum oscillations have been thoroughly discussed in Ref. [20] which is a common feature of the inverted band structure in InAs/GaSb bilayers and related materials [25–27].

Referring to Fig. 1(b), at the critical B field where the two unhybridized LLs cross, the bulk gap collapses and then a metallic conduction peak emerges, manifesting a topological phase transition from a QSHI to a NI. Two accompanying integer quantum Hall (IQH) states (ii) and (iii) as described in Fig. 1(b) are also observed, which have the opposite Chern numbers as shown by the blue and red dashed lines in Fig. 2(a). They merge into the standard QH sequence at high magnetic fields and their Chern numbers (the filling factors) can be determined by invoking the Streda formula [28]. (More detailed information can be found in the SM [17].)

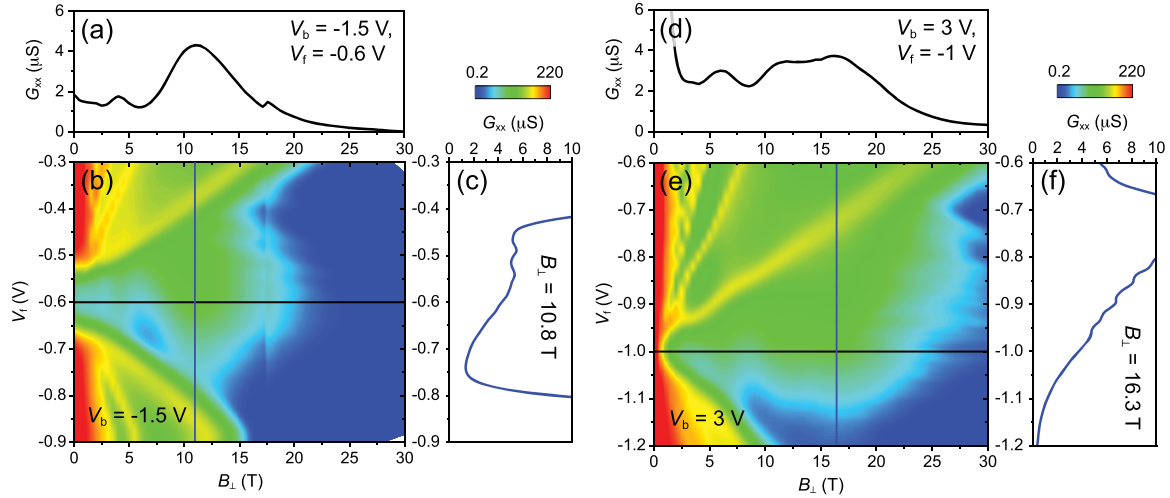


FIG. 3. The magneto-induced phase transitions under different band inversions. Two respective bulk conductivity maps are plotted at (b) $V_b = -1.5$ V and (e) $V_b = 3$ V. Corresponding conductance traces (horizontal linecuts) extracted with the Fermi energy pinned at the CNP are shown (a) at $V_f = -0.6$ V ($n = p \sim 1.24 \times 10^{11}$ cm $^{-2}$) and (d) at $V_f = -1$ V ($n = p \sim 2.48 \times 10^{11}$ cm $^{-2}$), respectively. Vertical line cuts are plotted to present bulk conductance at the transition point (c) at $B_{\perp} = 10.8$ T and (f) at $B_{\perp} = 16.3$ T.

A question one may reasonably ask is whether the BCP at 12 T coincides with the in-gap oscillations. A density relevant to the oscillations, $n_{\text{cross}} = 1.63 \times 10^{11}$ cm $^{-2}$, can be used to estimate the crossing field of the LLs: $B_c = 2n_{\text{cross}}h/e = 13.5$ T. This value is roughly consistent with that of the observed 12 T, although several factors may be considered. First, the nonparabolic band dispersions of both bands in a high magnetic field may contribute to the discrepancy. Perhaps more interestingly, deviation from the predicted critical field (13.5 T) may result from the quasimetallic regime due to e - h weak coupling in InAs/GaSb bilayer and the disorder effect [16].

Furthermore, tracing the conductance peak in Fig. 2(a), a “real” peak (rather than, e.g., a saddle point), which peaks not only along the magnetic field axis but also the gate voltage axis, is captured as marked by the red dashed box. It indicates that the bulk gap closes only at one point over the whole gap region in the phase diagram. These observations are fully consistent with a topological phase transition from a QSHI to a NI depicted in Fig. 1(b). It also reveals the relation between the BCP and the in-gap oscillations. The former arises from the gap closure due to the crossing of two unhybridized LLs, which is topologically protected while the latter is led by magnetic-field-induced modification of the energy gap when the e - h band hybridization is not strong enough to push the rest of the LLs out of the gap.

V. CORRELATION-DRIVEN SPONTANEOUS SYMMETRY BREAKING

Further examining the temperature dependence in Fig. 2(c), we observe certain abnormalities at the transition point. By extracting the thermal activation gap at different B_{\perp} as shown in Fig. 2(d), we found that the energy gap Δ reaches a dip around 12.5 T but does not entirely close. Several factors may contribute to the gap opening although its nature has not been well understood. Such gap closure

at the topological phase transition is normally symmetry protected. The spatial asymmetries including BIA and SIA are usually negligible in InAs/GaSb QWs [21]. But those effects really depend on the specific QW geometry and the external electric field, which may lead to a hybridization gap. On the other hand, electron-hole interaction may contribute to the gap opening as well since our sample lives in the regime where single-particle hybridization and excitonic interaction are competing. And the spatial inhomogeneity caused by fluctuations in electrostatic potential or variations in the thickness of the QW can also attribute to the gap opening at the transition point. Similar phenomena that the gap does not close during the topological phase transition are also reported in a similar InAs/InGaSb system [29] and a two-dimensional material system [5].

A new mini-gap Δ^* reminiscent of the excitonic gap [8,9] is observed at low temperatures. It emerges at around 9 T and increases with the magnetic field. The different positions of the Δ dip and the Δ^* peak in the magnetic axis may indicate their distinctive mechanisms. It is likely that the Δ^* arises from excitonic binding between the electrons and holes around the crossing point. It may persist even in the weakly noninverted regime as long as the binding energy is larger than the band gap [30–33], while the single-particle gap is supposed to close at the transition point (i.e., ~ 13 T).

Next, we investigate the transition under different band inversions. Figures 3(b) and 3(e) show the bulk conductance maps as a function of V_f and B_{\perp} at $V_b = -1.5$ V and $V_b = 3$ V, respectively. At the CNP, different V_b means different built-in electric fields and different degrees of the band inversion. At $V_b = -1.5$ V, where the bands are relatively shallowly inverted, it shows an unambiguous phase transition from an inverted band insulator (characterized by the in-gap oscillations) to a new insulator with the square resistance up to 1 G Ω . At $V_b = 3$ V, a deeply inverted case, we observe a similar phase transition but with a widely broadening transition peak, which can be attributed to the weak

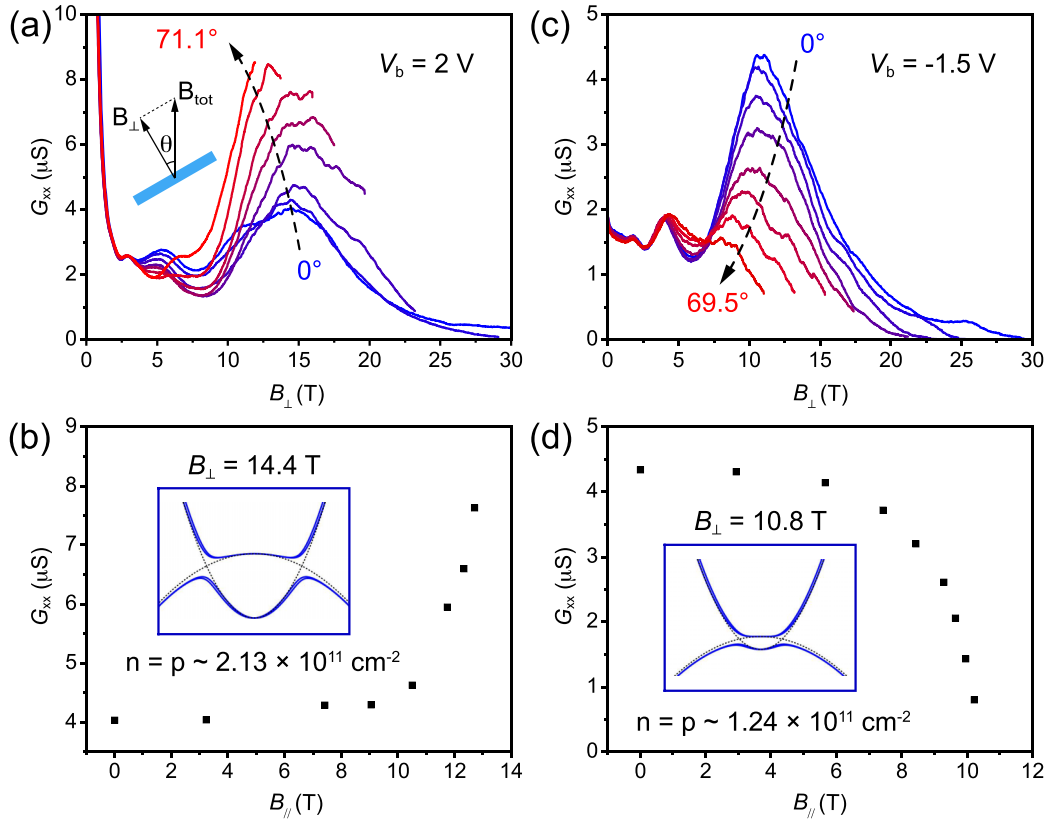


FIG. 4. The in-plane magnetic field dependence (a) at $V_b = 2$ V (deeply inverted regime), and (c) at $V_b = -1.5$ V (shallowly inverted regime). The corresponding peak conductance is extracted with B_{\perp} fixed (b) at 14.4 T ($V_b = 2$ V) and (d) at 10.8 T ($V_b = -1.5$ V).

hybridization and the band renormalization [15,16,34,35]. Comparing the magnetoconductance at the CNP, as shown in Figs. 3(a) and 3(d), the transition point for shallowly inverted bands arises at a lower magnetic field than that in a deeply inverted case, consistent with the phase transition picture.

Tuning the band inversion in the InAs/GaSb system also changes the interplay of the interlayer Coulomb interaction and the tunneling. In the shallowly inverted regime, the interaction effect is thought to be important to support a topological excitonic insulator [9]. We examine the in-plane magnetic field dependencies of the phase transition for different degrees of the band inversion. Figures 4(a) and 4(c) show the bulk magnetoconductance as a function of the tilt angle θ (defined in the inset) at $V_b = 2$ V and $V_b = -1.5$ V, respectively. In the deeply inverted regime ($V_b = 2$ V), the BCP is found to increase with the in-plane magnetic field $B_{\parallel} = B_{\text{tot}} \sin\theta$. For such a spatially separated e - h bilayer, applying B_{\parallel} is supposed to induce a relative momentum shift between two bands, $\Delta k = eB_{\parallel}\langle z \rangle/\hbar$, where $\langle z \rangle$ is the vertical distance between two layers [36]. This may close the hybridization gap and convert the QSH insulator into a semimetal. According to the extracted peak conductance as a function of B_{\parallel} at $B_{\perp} = 14.4$ T in Fig. 4(b), the transition point can be considered a metal at $B_{\parallel} = 13$ T where the BCP shows a rapid increase. The in-gap oscillations are also found to deviate from the original pattern under B_{\parallel} . It indicates that the in-plane field significantly changes the Fermi surface, which will not be affected if the gap is driven by excitonic interaction, further

supporting the single-particle-hybridization-dominant picture in the deeply inverted regime (a more detailed explanation can be found in the SM [17]).

An opposite trend of response to the in-plane magnetic field is found when the same device is tuned into the shallowly inverted regime ($V_b = -1.5$ V), where the transition peak is continuously suppressed when B_{\parallel} increases, and essentially disappears when $B_{\parallel} > 10$ T ($\theta > 71^\circ$), as shown in Fig. 4(d). It indicates that B_{\parallel} converts the gap-closing topological phase transition into a smooth crossover without gap closing. Such a crossover between two topologically distinctive phases has to be accompanied by symmetry breaking [5,10]. Here B_{\parallel} component reduces the interlayer tunneling and hence enhances the effective interaction strength U/A . Overall, the conductance suppression under B_{\parallel} in shallowly inverted InAs/GaSb bilayer suggests a correlation-driven state with spontaneous symmetry breaking before the transition. The robustness of the in-gap oscillations in a lower field supports this assertion as well.

VI. DISCUSSION AND CONCLUSION

The remainder of this paper will focus on more discussions on the exciton effect. For a dilute e - h system, long-range Coulomb interaction prefers to pair electrons and holes into a bosonic exciton condensate. The excitonic gap is weakly dependent on the momentum shift induced by an in-plane magnetic field and to some extent it is enhanced due to a suppression of e - h interlayer tunneling. We have observed two

well-separated regimes which can be parametrized by the degree of the band inversion. For the deeply inverted regime, as shown in Figs. 4(a) and 4(b), the gap closing at the transition point can be well explained within a single-particle model. For the shallowly inverted regime in Figs. 4(c) and 4(d), a smooth crossover without gap closing suggests a correlation-driven state with spontaneous symmetry breaking before the transition. All of these observations are consistent with the excitonic insulator instability mechanism in InAs/GaSb bilayer when considering the interplay between the Coulomb interaction and the hybridization [9,37]. More recently, a time-reversal-symmetry-broken state is theoretically proposed for InAs/GaSb bilayers [12], which emerges between the noninverted bands and the inverted bands where QSH insulators are observed. This regime exactly falls into the dilute limit where excitonic insulators [9,38] and the results in Figs. 4(c) and 4(d) are observed.

In conclusion, we observed a magneto-driven topological phase transition from a QSHI to a NI. Significantly, as the e - h system is tuned towards the shallowly inverted regime, long-range Coulomb interaction dominates and converts the topological phase transition into a smooth crossover without gap closing. It suggests a corre-

lated state with spontaneous symmetry breaking. Our work demonstrates a highly controllable e - h system under high magnetic fields to explore the interplay between topology and interaction.

ACKNOWLEDGMENTS

We gratefully acknowledge C. L. Yang and P. L. Li for technical assistance. The work at PKU was funded by the National Key R&D Program of China (Grants No. 2017YFA0303300 and No. 2019YFA0308400), by the Strategic Priority Research Program of Chinese Academy of Sciences (Grant No. XDB28000000), and the Innovation Program for Quantum Science and Technology (Grant No. 2021ZD0302600). The InAs/GaSb quantum well structures were prepared by molecular beam epitaxy by Gerard Sullivan. A portion of this work was performed at the National High Magnetic Field Laboratory, which was supported by the National Science Foundation Cooperative Agreement No. DMR-1157490 and the State of Florida. The work at UCAS was supported by the National Key R&D Program of China (Grant No. 2018YFA0305800) and the National Natural Science Foundation of China (Grant No. 12174387).

-
- [1] C. L. Kane and E. J. Mele, Z_2 topological order and the quantum spin hall effect, *Phys. Rev. Lett.* **95**, 146802 (2005).
- [2] M. König, S. Wiedmann, C. Brüne, A. Roth, H. Buhmann, L. W. Molenkamp, X.-L. Qi, and S.-C. Zhang, Quantum spin hall insulator state in HgTe quantum wells, *Science* **318**, 766 (2007).
- [3] I. Knez, R. R. Du, and G. Sullivan, Evidence for helical edge modes in inverted InAs/GaSb quantum wells, *Phys. Rev. Lett.* **107**, 136603 (2011).
- [4] S. Wu, V. Fatemi, Q. D. Gibson, K. Watanabe, T. Taniguchi, R. J. Cava, and P. Jarillo-Herrero, Observation of the quantum spin hall effect up to 100 kelvin in a monolayer crystal, *Science* **359**, 76 (2018).
- [5] T. Li, S. Jiang, B. Shen, Y. Zhang, L. Li, Z. Tao, T. Devakul, K. Watanabe, T. Taniguchi, L. Fu, J. Shan, and K. F. Mak, Quantum anomalous hall effect from intertwined moiré bands, *Nature (London)* **600**, 641 (2021).
- [6] B. A. Bernevig, T. L. Hughes, and S.-C. Zhang, Quantum spin hall effect and topological phase transition in HgTe quantum wells, *Science* **314**, 1757 (2006).
- [7] C. L. Kane and E. J. Mele, Quantum spin hall effect in graphene, *Phys. Rev. Lett.* **95**, 226801 (2005).
- [8] L. Du, I. Knez, G. Sullivan, and R.-R. Du, Robust helical edge transport in gated InAs/GaSb bilayers, *Phys. Rev. Lett.* **114**, 096802 (2015).
- [9] L. Du, X. Li, W. Lou, G. Sullivan, K. Chang, J. Kono, and R.-R. Du, Evidence for a topological excitonic insulator in InAs/GaSb bilayers, *Nat. Commun.* **8**, 1971 (2017).
- [10] F. Xue and A. H. MacDonald, Time-reversal symmetry-breaking nematic insulators near quantum spin hall phase transitions, *Phys. Rev. Lett.* **120**, 186802 (2018).
- [11] Y. Zeng, F. Xue, and A. H. MacDonald, In-plane magnetic field induced density wave states near quantum spin hall phase transitions, *Phys. Rev. B* **105**, 125102 (2022).
- [12] T. Paul, V. F. Becerra, and T. Hyart, Interplay of quantum spin hall effect and spontaneous time-reversal symmetry breaking in electron-hole bilayers. I. transport properties, *Phys. Rev. B* **106**, 235420 (2022).
- [13] T. Paul, V. F. Becerra, and T. Hyart, Interplay of quantum spin hall effect and spontaneous time-reversal symmetry breaking in electron-hole bilayers. II. zero-field topological superconductivity, *Phys. Rev. B* **106**, 235421 (2022).
- [14] F. Qu, A. J. A. Beukman, S. Nadj-Perge, M. Wimmer, B.-M. Nguyen, W. Yi, J. Thorp, M. Sokolich, A. A. Kiselev, M. J. Manfra, C. M. Marcus, and L. P. Kouwenhoven, Electric and magnetic tuning between the trivial and topological phases in InAs/GaSb double quantum wells, *Phys. Rev. Lett.* **115**, 036803 (2015).
- [15] L. Du, T. Li, W. Lou, X. Wu, X. Liu, Z. Han, C. Zhang, G. Sullivan, A. Ikhlassi, K. Chang, and R.-R. Du, Tuning edge states in strained-layer InAs/GaInSb quantum spin hall insulators, *Phys. Rev. Lett.* **119**, 056803 (2017).
- [16] D. I. Pikulin, T. Hyart, S. Mi, J. Tworzydło, M. Wimmer, and C. W. J. Beenakker, Disorder and magnetic-field-induced breakdown of helical edge conduction in an inverted electron-hole bilayer, *Phys. Rev. B* **89**, 161403(R) (2014).
- [17] See Supplemental Material at <http://link.aps.org/supplemental/10.1103/PhysRevResearch.6.023192> for technical details and additional discussions.
- [18] C. Liu, T. L. Hughes, X.-L. Qi, K. Wang, and S.-C. Zhang, Quantum spin hall effect in inverted type-II semiconductors, *Phys. Rev. Lett.* **100**, 236601 (2008).
- [19] X. Mu, G. Sullivan, and R.-R. Du, Effective g-factors of carriers in inverted InAs/GaSb bilayers, *Appl. Phys. Lett.* **108**, 012101 (2016).
- [20] Z. Han, T. Li, L. Zhang, G. Sullivan, and R.-R. Du, Anomalous conductance oscillations in the hybridization gap of InAs/GaSb quantum wells, *Phys. Rev. Lett.* **123**, 126803 (2019).

- [21] C. Liu and S. Zhang, Models and materials for topological insulators, in *Topological Insulator*, edited by M. Franz and L. W. Molenkamp (Elsevier, New York, 2013), Vol. 6.
- [22] L. Zhang, X.-Y. Song, and F. Wang, Quantum oscillation in narrow-gap topological insulators, *Phys. Rev. Lett.* **116**, 046404 (2016).
- [23] J. C. Y. Teo, L. Fu, and C. L. Kane, Surface states and topological invariants in three-dimensional topological insulators: Application to $\text{Bi}_{1-x}\text{Sb}_x$, *Phys. Rev. B* **78**, 045426 (2008).
- [24] L. Fu, Topological crystalline insulators, *Phys. Rev. Lett.* **106**, 106802 (2011).
- [25] D. Xiao, C.-X. Liu, N. Samarth, and L.-H. Hu, Anomalous quantum oscillations of interacting electron-hole gases in inverted Type-II InAs/GaSb quantum wells, *Phys. Rev. Lett.* **122**, 186802 (2019).
- [26] Z. Xiang, Y. Kasahara, T. Asaba, B. Lawson, C. Tinsman, L. Chen, K. Sugimoto, S. Kawaguchi, Y. Sato, G. Li, S. Yao, Y. L. Chen, F. Iga, J. Singleton, Y. Matsuda, and L. Li, Quantum oscillations of electrical resistivity in an insulator, *Science* **362**, 65 (2018).
- [27] L. Liu, Y. Chu, G. Yang, Y. Yuan, F. Wu, Y. Ji, J. Tian, R. Yang, K. Watanabe, T. Taniguchi, G. Long, D. Shi, J. Liu, J. Shen, L. Lu, W. Yang, and G. Zhang, Quantum oscillations in field-induced correlated insulators of a moiré superlattice, *Sci. Bull.* **68**, 1127 (2023).
- [28] A. H. MacDonald, Introduction to the physics of the quantum Hall regime, [arXiv:cond-mat/9410047](https://arxiv.org/abs/cond-mat/9410047).
- [29] H. Irie, T. Akiho, F. Couëdo, K. Suzuki, K. Onomitsu, and K. Muraki, Energy gap tuning and gate-controlled topological phase transition in InAs/ $\text{In}_x\text{Ga}_{1-x}\text{Sb}$ composite quantum wells, *Phys. Rev. Mater.* **4**, 104201 (2020).
- [30] N. F. Mott, The transition to the metallic state, *Philos. Mag.* **6**, 287 (1961).
- [31] W. Kohn, Excitonic phases, *Phys. Rev. Lett.* **19**, 439 (1967).
- [32] D. Jérôme, T. M. Rice, and W. Kohn, Excitonic insulator, *Phys. Rev.* **158**, 462 (1967).
- [33] B. I. Halperin and T. M. Rice, Possible anomalies at a semimetal-semiconductor transition, *Rev. Mod. Phys.* **40**, 755 (1968).
- [34] I. Knez, R. R. Du, and G. Sullivan, Finite Conductivity in mesoscopic hall bars of inverted InAs/GaSb quantum wells, *Phys. Rev. B* **81**, 201301(R) (2010).
- [35] Y. Naveh and B. Laikhtman, Magnetotransport of coupled electron-holes, *Europhys. Lett.* **55**, 545 (2001).
- [36] M. J. Yang, C. H. Yang, B. R. Bennett, and B. V. Shanabrook, Evidence of a hybridization gap in “Semimetallic” InAs/GaSb systems, *Phys. Rev. Lett.* **78**, 4613 (1997).
- [37] D. I. Pikulin and T. Hyart, Interplay of exciton condensation and the quantum spin hall effect in InAs/GaSb bilayers, *Phys. Rev. Lett.* **112**, 176403 (2014).
- [38] R. Wang, T. A. Sedrakyan, B. Wang, L. Du, and R.-R. Du, Excitonic topological order in imbalanced electron-hole bilayers, *Nature (London)* **619**, 57 (2023).